ELSEVIER

Atmospheric Research 46 (1998) 293–305

ATMOSPHERIC RESEARCH

On the potential importance of sulfur-induced activation of soot particles in nascent jet aircraft exhaust plumes [1]

B. Kärcher

Lehrstuhl für Bioklimatologie und Immissionsforschung, Universität München, Freising, Germany

Abstract

The chemical conversion of emitted SO_2 and SO_3 to gaseous H_2SO_4 in nascent aircraft exhaust plumes and subsequent adsorption of the fully oxidized sulfur species on the surfaces of emitted combustion aerosols (soot) is investigated. Results are presented for the mass fractions of SO_3 and H_2SO_4 acquired per soot particle early in the plume, suggesting that sulfur-induced activation is an efficient pathway to increase the ability of exhaust soot emitted at altitude to host heterogeneous chemical reactions and to trigger the formation of cirrus clouds. © 1998 Elsevier Science B.V.

Keywords: Aircraft sulfur emissions; Soot activation; Particle formation

1. Introduction

The possible impact of jet aircraft emissions on global chemistry and climate is currently investigated in several research programs (World Meteorological Organization, 1995). A particularly important part of this research is devoted to the emission and formation of particulate matter. It seems well established that new volatile liquid aerosols, composed of H_2SO_4 and H_2O just like the particles in the stratospheric background aerosol layer, are formed by binary homogeneous nucleation in young exhaust plumes. Aircraft engines also emit nonvolatile combustion aerosols (soot) that may serve as heterogeneous freezing nuclei and may therefore lead to an increase in the cirrus formation frequency in upper tropospheric flight corridors (Jensen and Toon, 1997). It is essential to have detailed knowledge about physico–chemical properties of

[1] This paper is dedicated to Professor Peter Fabian on the occasion of his 60th anniversary.

PII S0169-8095(97)00070-7

soot particles emitted by aircraft to evaluate their potential to host heterogeneous chemical reactions (Kärcher and Peter, 1995). Jet aircraft are the major anthropogenic source of soot particles in the upper troposphere and lower stratosphere (Blake and Kato, 1995).

A few investigations concerning the cloud-condensation nuclei (CCN) properties or ice-forming abilities of soot have been published, indicating a large range of CCN/CN ratios of soot ranging from 1/1000 (Pitchford et al., 1991) to 1/3 (Whitefield et al., 1993). This large uncertainty probably reflects the effect of different soot sources and experimental conditions. Blake and Kato (1995) discussed far-field effects of black carbon in the upper troposphere and lower stratosphere and concluded that aircraft soot probably does not represent a significant source of CN for H_2SO_4/H_2O aerosols. On the other hand, Wyslouzil et al. (1994) have observed a very marked increase in H_2O adsorption on model carbon particles that were treated with H_2SO_4 compared to untreated particles, at least in qualitative agreement with an analysis of the wetting behavior of graphitic carbon under plume conditions (Kärcher et al., 1996a).

In this paper, we present arguments by which we support the notion that aircraft soot emitted at altitude does contain soluble material stemming from interaction with gaseous exhaust sulfur species in the nascent jet plume. We focus on the adsorption of fully oxidized sulfur species, S(VI), on the surfaces of the soot particles for several reasons. (1) In laboratory experiments, Wyslouzil et al. (1994) observed hydration of carbon aerosols under water subsaturated conditions after treatment of the carbon particles with H_2SO_4. (2) Whitefield et al. (1993) noted a correlation between soluble mass fractions found on fresh soot taken from the hot exhaust directly behind jet engines with the fuel-sulfur content. (3) It is known that substantial fractions (2–20%) of the fuel sulfur $SO_x (= SO_2 + SO_3)$ are emitted in the form of SO_3 (Hunter, 1982; Harris, 1990). This issue has very recently been investigated by modeling of combustion kinetics in gas turbines (Brown et al., 1996); their simulations also allow for some minor emissions of H_2SO_4 and suggest a nonlinear dependence of SO_3 production on the total fuel-sulfur content. (4) The sticking probability of SO_2 on soot appears to be too small to be relevant (Rogaski et al., 1997) and the heterogeneous oxidation of SO_2 to S(VI), even in the presence of catalysts such as NO_2, is probably too slow to be efficient on the short time scales for soot activation in the young exhaust plume. In contrast, SO_3 will easily be oxidized heterogeneously to H_2SO_4. (5) Using the liquid H_2SO_4/H_2O soot coating assumption, we could explain the buildup of a visible water ice contrail under threshold formation conditions (Kärcher et al., 1996a). For the second and fifth reasons, we focus on the activation of soot particles between the core engine exit plane and prior to visible contrail formation (the latter occurring at plume age t around 0.1 s). Scavenging of the newly formed H_2SO_4/H_2O droplets (generated by homogeneous nucleation at similar plume ages of 0.1 s) by soot could lead to additional sulfur coatings on the surfaces of exhaust soot, as estimated by Brown et al. (1996) and Kärcher et al. (1996a).

We first focus on the chemical conversion of emitted SO_x into gaseous sulfuric acid to evaluate the number of S(VI) molecules present in the gas phase (Section 2). We present a simple analytical model describing adsorption of gaseous exhaust species on the surfaces of the emitted soot particles in the diluting exhaust plume (Section 3). The paper continues with a discussion of the maximum sulfur mass fractions that can be

adsorbed by aircraft soot in the nascent exhaust plume (Section 4), where implications for aircraft-induced volatile aerosol formation and soot-induced formation of cirrus clouds are also given. Section 5 summarizes the basic conclusions of this work.

2. Sulfur-conversion efficiency

We use a detailed chemical model (Kärcher et al., 1996b) to evaluate the sulfur oxidation kinetics in the nascent exhaust plume, i.e., after the exhaust gases exited the jet engines. In the following, the subscript 0 indicates initial values taken at the nozzle exit plane (plume age $t = 0$). We note that the chemical reactions take place in the diluting aircraft wake. Plume dilution is driven by turbulent entrainment of ambient air.

As a representative example, we investigate the transformation of emitted SO_x to H_2SO_4 in the wake of the subsonic Airbus A 310. The time scale of the gas-phase reactions that lead to the buildup of H_2SO_4 from exhaust SO_2 is determined by the emitted hydroxyl radical OH, which initializes the oxidation of SO_2, and by the reaction of SO_3 with emitted H_2O. In detail, the reaction mechanism reads (Stockwell and Calvert, 1983; Frenzel and Arnold, 1994):

$$\begin{aligned} SO_2 + OH + M &\rightarrow HSO_3 + M \\ HSO_3 + O_2 &\rightarrow HO_2 + SO_3 \\ SO_3 + nH_2O + M &\rightarrow H_2SO_4 \cdot (H_2O)_{n-1} + M \end{aligned}$$

where M denotes a chemically passive reaction partner. According to Stockwell and Calvert (1983), $n = 1$, but H_2SO_4 production could also involve water dimer molecules ($n = 2$, see Brown et al., 1996). Possible differences in the rate constants are not important under plume conditions. When no SO_3 is emitted, oxidation of SO_2 by OH builds up a transient steady-state level of SO_3 that quickly reacts with H_2O to form H_2SO_4 within a few milliseconds after the exhaust exited the engines. In this way, depending on $[OH]_0$, typical SO_2 to H_2SO_4 conversion efficiencies $[H_2SO_4]_{max}/[SO_2]_0 < 1$–2% are reached until OH is depleted by concomitant reactions with emitted NO_x (Miake-Lye et al., 1994; Kärcher et al., 1996b).

We extend these studies and investigate the maximum SO_x to H_2SO_4 conversion efficiencies, $\eta(s, [OH]_0) = [H_2SO_4]_{max}/[SO_x]_0$, as a function of $s = [SO_3]_0/[SO_x]_0$ and for several values of $[OH]_0$, see Fig. 1. Note that this definition of η only addresses transformation in the gas phase and does not take into account possible heterogeneous losses on soot as discussed in Section 3. The amount of SO_3 at the nozzle exit plane, $[SO_3]_0$, is generated within the jet engines by reactions involving SO_x and atomic oxygen, the latter being controlled by the combustion of CO. Because we do not address the high-temperature chemical processes within the engines, $[SO_3]_0$, or s, is varied as a free parameter.

In the limit $s \rightarrow 0$, H_2SO_4 production is initiated by the oxidation of SO_2 as noted above, and the dependence $\eta([OH]_0)$ is identical to that discussed previously (Kärcher et al., 1996b). The rate-limiting reaction of SO_2 with OH causes η to be bound between 0.01% and 0.5% for low (dotted line) to rather high (solid line) $[OH]_0$ levels. With

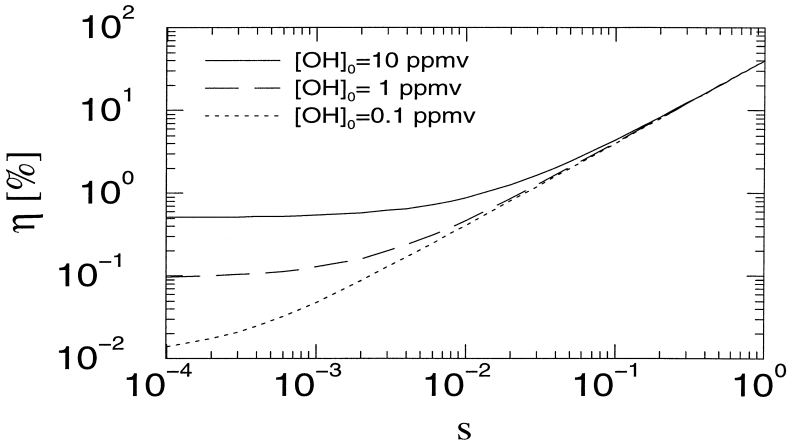

Fig. 1. Maximum conversion efficiency $\eta = [H_2SO_4]_{max} / [SO_x]_0$ of emitted SO_x to H_2SO_4 vs. the exit plane ratio $s = [SO_3]_0 / [SO_x]_0$ for various values of emitted OH in the jet plume of an Airbus A 310. For $s < 10^{-2}$ the production of H_2SO_4 is limited by the available exhaust OH, but becomes very efficient for $s > 10^{-2}$.

increasing amount of directly emitted SO_3, η increases because the fast reaction of SO_3 with H_2O immediately leads to H_2SO_4 and bypasses the slower $SO_2 + OH$ reaction pathway. For $s < 10^{-2}$, η shows a pronounced $[OH]_0$ dependence, because the SO_3 concentration produced in the plume via $SO_2 + OH$ is greater than, or at least similar to, the emitted SO_3. However, for $s > 10^{-2}$, η increases substantially because direct conversion of $[SO_3]_0$ to H_2SO_4 takes over the dominant part and the $[OH]_0$ dependence diminishes. In this case, the production of gaseous H_2SO_4 becomes very efficient and is no longer constrained by the available exhaust OH. Complete oxidation of fuel sulfur to SO_3 in the jet engines ($s = 1$) would result in a maximum conversion efficiency of 40% for the A 310, see Fig. 1. Note that $\eta = 100\%$ is not reached since mixing reduces the SO_3 concentration while being converted to H_2SO_4. Consequently, conversion efficiencies can even be somewhat higher in aircraft plumes with slower mixing in the jet regime, but similar emission speciation, compared to the A 310.

3. Soot and sulfur interaction

We now focus on the adsorption of gaseous exhaust species on the surfaces of emitted soot particles which are assumed to be spherical. Surface roughness features or a nonspherical (possibly fractal) shape that might enhance the specific surface area of the fresh soot are neglected due to the lack of more detailed information. The assumptions about size, number density, and radial size distribution of exhaust soot we employ in this work are motivated by field-sampling experiments of combustion aerosols by Hagen et al. (1992) and are consistent with the current typical range of the soot emission index, EI(soot) = 0.1–1 g soot per kg fuel burnt, cf. Schumann et al. (1996). It is important to estimate how much of the emitted SO_3 can be taken up by soot instead of being

chemically converted to H_2SO_4 in the gas phase, as assumed above for the discussion of η. Similarly, we need to know how many H_2SO_4 molecules are adsorbed and therefore not available for binary homogeneous nucleation. The adsorption rates of SO_3 and H_2SO_4 on the small ($\sim$ 20 nm) soot particles will be taken from gas kinetic theory. This maximizes predicted adsorption rates and sets an upper boundary for the binary heterogeneous nucleation rate of H_2SO_4 and H_2O on soot. We will develop a simple analytical model to treat the adsorption in the diluting jet plume which can be easily applied to engine/wake conditions not discussed in the present paper. For this model, we assume that molecules are emitted with a number density n_0 and consider only dilution and adsorption as sink processes for the molecular number densities.

Upon striking the soot surface, molecules (number density n) are adsorbed according to a sticking probability $\gamma \leq 1$ and only a fraction f remains in the gas phase. Vapor species (ambient concentration n_a) and soot (number density n_s) dilute in the jet plume, driven by the entrainment rate $\omega(t)$. To determine $f(t)$, we consider the equation

$$\frac{dn}{dt} = -\omega(n - n_a) - \beta A_s, \; \beta = \frac{\gamma}{4} n \bar{v}, \tag{1}$$

whereby $\beta(t)$ is the impingement rate per second per unit surface area of soot, $\bar{v}$ is the thermal velocity of the molecules, and $A_s(t) = 4\pi r_s^2 n_s(t) \exp(2\ln^2 \sigma_s)$ is the soot surface area density, with the mean radius r_s and modal width σ_s of the assumed log-normal size distribution. According to Hagen et al. (1992) and Schumann et al. (1996), $n_s = 10^6$–10^7 cm^{-3}, $r_s = 10$–30 nm, and $\sigma_s \simeq 1.4$. Eq. (1) approximately describes the competition between mixing (first term on the right side) and adsorption (second term) in the jet regime, i.e., for plume ages $t < 10$ s. (It strictly holds only for mixing ratios, see Kärcher, 1995). The characteristic time scales are

$$t_m = \frac{1}{\omega_{max}}, \; t_{ad} = \frac{4}{\gamma \bar{v} A_{s,0}}, \; \tau = \frac{t_m}{t_{ad}}, \tag{2}$$

respectively, which we combine to the single key parameter τ. Typical values t_m are of the order of 10 ms. We use $\gamma = 1$ and $\bar{v} = 2.5 \times 10^4$ cm s^{-1}, and assume $n(t) \gg n_a$ and neglect entrainment of ambient soot particles ($n_{s,a} = 0$), which is a good approximation in the early stage of plume dilution. (Lower γ-values could be numerically compensated by an enhanced specific surface area resulting from the fractal structure of soot.) The mixing rate can well be approximated by

$$\omega = \begin{cases} 0 & : \quad t \leq t_m \\ \alpha / t & : \quad t > t_m \end{cases}, \tag{3}$$

with $\alpha \leq 1$. Typical values for α in the plume near-field range from 0.8 to 1. Coagulation between soot particles is slow compared to dilution as long as $n_{s,0} < 4 \times 10^7$ cm^{-3}, assuming Brownian coagulation (Fuchs, 1964). However, thermal coagulation could be enhanced since a possible nonspherical shape of the emitted soot might lead to more efficient scavenging due to an enhanced probability of close encounters that lead

to scavenging. Hence, the evolution of the soot number density is given by $\mathrm{d}n_s/\mathrm{d}t = -\omega n_s$, or

$$n_s(t) = n_{s,0} D(t), \tag{4}$$

with the overall dilution rate $D \leq 1$ (Kärcher, 1995)

$$D(t) = \exp\left(-\int_0^t \omega(t)\mathrm{d}t \right) = \begin{cases} 1 & : \quad t \leq t_m \\ (t_m/t)^{\alpha} & : \quad t > t_m. \end{cases} \tag{5}$$

With these assumptions, the loss Eq. (1) for n can be integrated analytically. The solution reads

$$n(t) = n_0 D(t) \exp\left[-\tau\phi(t) \right], \tag{6}$$

with the initial vapor number density $n(t=0) = n_0$ at the engine exit plane and the function

$$\phi(t) = \frac{1}{t_m}\int_0^t D(t)\mathrm{d}t = \begin{cases} t/t_m & : \quad t \leq t_m \\ 1 + \left[(t/t_m)^{1-\alpha} - 1 \right]/(1-\alpha) & : \quad t > t_m \text{ and } \alpha < 1 \\ 1 + \ln(t/t_m) & : \quad t > t_m \text{ and } \alpha = 1. \end{cases} \tag{7}$$

Introducing the dimensionless time $\theta = t/t_m$, the fraction of molecules that remain in the gas phase and are not yet adsorbed by the soot particles at time θ is given by

$$f_\tau(\theta) = \exp\left[-\tau\phi(\theta) \right]. \tag{8}$$

Likewise it can be shown that the solution for the number density of molecules that are already adsorbed by soot at the plume age t, $n_c(t)$, which follows from

$$\frac{\mathrm{d}n_c}{\mathrm{d}t} = -\omega n_c + \beta A_s, \tag{9}$$

can be cast into the simple form

$$n_c = n_0 D(t) \tau \psi_\tau(t), \; \psi_\tau(\theta) = \left[1 - f_\tau(\theta) \right]/\tau. \tag{10}$$

If we define $\delta(t)$ as the actual thickness of the adsorbed layer and δ_{ML} as the thickness of one monolayer, the number of adsorbed monolayers $\mathrm{ML}(t) = \delta(t)/\delta_{ML}$ can then be estimated from the mass balance equation $A_s(t)\delta(t) = \upsilon n_c(t)$, where $A_s(t) = A_{s,0} D(t)$ and υ is the specific molecular volume of the adsorbed molecules, yielding

$$\mathrm{ML}(\theta) = \frac{\beta_0 t_m}{\sigma} \psi_\tau(\theta). \tag{11}$$

The ratio $\sigma = \delta_{ML}/\upsilon$ is the average number of sites per unit area of soot surface ($\sigma \simeq 5 \times 10^{14}$ cm^{-2}).

The universal functions $f_\tau(\theta)$ and $\psi_\tau(\theta)$ are displayed in Figs. 2 and 3, respectively, for various values of τ for $\alpha = 0.9$ vs. the scaled plume age θ. Results for any particular

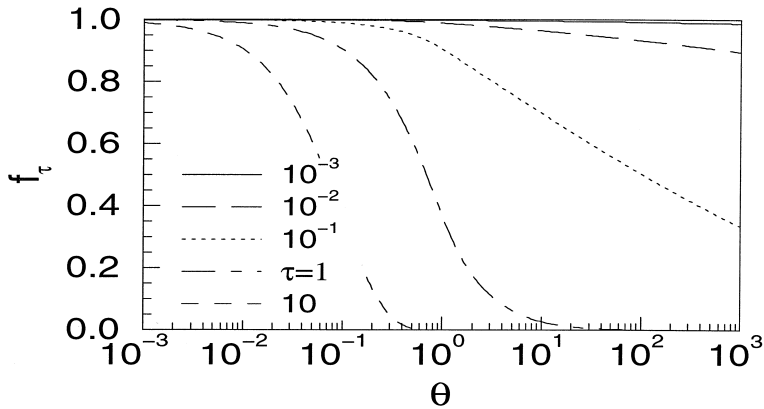

Fig. 2. Fraction f_τ of molecules that remain in the gas phase and are not adsorbed by soot vs. the scaled plume age θ. Eq. (8) is displayed for $\alpha = 0.9$. The parameter $\tau = t_m / t_{ad}$ is the ratio of mixing to adsorption time scale, cf. Eq. (2). For $\tau > 1$ ($\tau < 1$), adsorption is faster (slower) than plume dilution due to entrainment of ambient air.

problem can be read off these general solutions after conversion to the scaled variables τ and θ. If adsorption is faster than mixing ($\tau > 1$), f_τ decreases and ψ_τ increases rapidly; otherwise ($\tau < 1$), a large fraction of molecules remains in the gas phase and will not be taken up by the soot particles in the early plume, because both the number densities of soot and vapor molecules are reduced due to fast mixing which counteracts adsorption. Note the weak variations of f_τ and ψ_τ when $\tau < 10^{-2}$.

We finally estimate the mass fraction μ of adsorbed SO_3 and H_2SO_4 molecules per soot particle. The chemical conversion of SO_3 to H_2SO_4 in the gas phase by the reaction with H_2O is completed in typically $t_1 = 20$ ms. Sulfuric acid in turn becomes depleted

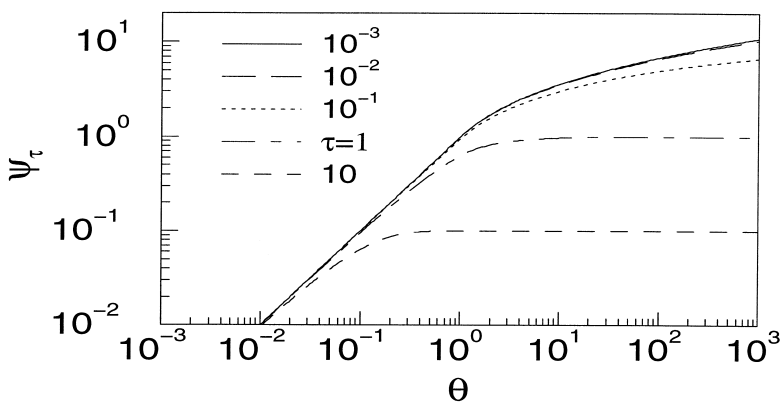

Fig. 3. Number of adsorbed monolayers ψ_τ (normalized by the characteristic value $\beta_0 t_m / \sigma$, see text) from Eqs. (10) and (11) for $\alpha = 0.9$ vs. the scaled plume age θ. As in Fig. 2, τ is the ratio of time scales due to mixing and adsorption. In the fast mixing case $\tau > 1$, ψ_τ saturates early, since essentially all the emitted vapor molecules are adsorbed early in the plume. In these cases, the fraction f_τ of molecules remaining in the gas phase shown in Fig. 2 rapidly decrease for $\theta < 1$. Note that the total number of adsorbed molecules scales $\propto \tau\psi_\tau$.

by binary homogeneous nucleation which typically sets in at plume ages $t_2 = 0.1$ s; t_2 may vary by about a factor 2 according to our nucleation simulations, depending on the cooling rate in the jet plume that mainly controls the evolution of the nucleation rate. For plume ages greater than t_1 (for SO_3) and t_2 (for H_2SO_4), these species vanish from the gas phase and can no longer be adsorbed. For this reason, we evaluate Eq. (10) separately for SO_3 at $\theta_1 = t_1/t_m$ and for H_2SO_4 at $\theta_2 = t_2/t_m$, since Eq. (10) is not valid beyond these plumes ages (chemical depletion of SO_3 and nucleation losses of H_2SO_4 have been neglected in deriving Eq. (10)). This will yield upper bounds for the mass fractions acquired past exit. Using the abbreviations $a_\tau(\theta_1) = [1 - f_\tau(\theta_1)]$ and $a_\tau(\theta_2) = [1 - f_\tau(\theta_2)]$ for the fractions of adsorbed vapor molecules, Eq. (10) yields for the mass m_{ad} of SO_3 and H_2SO_4 on the soot particles

$$m_{ad} = \underbrace{M_1 n_0 \mathcal{D} s a_\tau(\theta_1)}_{\text{from } SO_3} + \underbrace{M_2 n_0 \mathcal{D} \eta(s) a_\tau(\theta_2)}_{\text{from } H_2SO_4}, \tag{12}$$

where $M_1 = 80$ g mol^{-1} and $M_2 = 98$ g mol^{-1} are the molar masses of SO_3 and H_2SO_4, $n_0 \equiv [SO_x]_0$ denotes the total number of SO_x molecules at the engine exit, and where we made use of the definitions of s and η as given in Section 2. Sulfur molecules could already be taken up in the combustor and lead to an additional increase in m_{ad}. However, this fraction is unknown and probably small due to the high combustion temperatures; its effects on μ discussed in Section 4 could be masked by uncertainties in the prescribed values for s. Defining the average molecular mass of emitted SO_2 and SO_3 molecules by $M(s) = 64(1 - s) + 80s$ g mol^{-1}, introducing the dimensionless functions $b_1(s) = M_1/M = 1/[0.8(1 - s) + s]$ and $b_2(s) = M_2/M = 1/[0.65(1 - s) + 0.82s]$, and dividing Eq. (12) by the total soot mass per cm^3 air, $m_s = 4\pi\rho_s r_s^3 n_{s,0} D/3$ (mass density $\rho_s \simeq 2$ g cm^{-3}), we find for $\mu = m_{ad}/m_s$

$$\mu = \frac{\mathrm{EI}(SO_x)}{\mathrm{EI}(\mathrm{soot})}\left[s b_1(s) a_\tau(\theta_1) + \eta(s) b_2(s) a_\tau(\theta_2)\right], \tag{13}$$

with the SO_x emission index $\mathrm{EI}(SO_x) = n_0 M(s)$. We set $\mathrm{EI}(SO_x)$ twice the total fuel-sulfur emission index EI(S), for simplicity. Average fuel-sulfur contents range between EI(S) = 0.1–1 g S per kg fuel (e.g., Schumann et al., 1996).

4. Discussion and implications

We evaluate Eq. (13) for three different, general types of mixing specifications and soot micro-physical properties. We emphasize that the spherical approximation for the shape of the soot particles and the prescribed log-normal size distribution are at most best guesses, since a comprehensive characterization of fresh soot emitted at altitude is still lacking. Type 1 is characterized by fast mixing ($\alpha = 0.8$, $t_m = 3$ ms) and an exit plane soot number density ($n_{s,0} = 5 \times 10^6$ cm^{-3}) with rather large average particle size ($r_s = 30$ nm). Type 2 is chosen to be an intermediate case with $\alpha = 0.9$, $t_m = 10$ ms, $n_{s,0} = 10^7$ cm^{-3}, and $r_s = 20$ nm. Type 3 is characterized by slow mixing ($\alpha = 1$, $t_m = 50$ ms) and high emissions ($n_{s,0} = 4 \times 10^7$ cm^{-3}) of rather small soot particles

Table 1
Soot emission indices EI(soot), ratio τ of mixing to adsorption time scale, scaled plume age past exit θ_1 when SO_3 is completely converted to H_2SO_4, scaled plume age θ_2 indicating the onset of binary homogeneous nucleation that eventually depletes gaseous H_2SO_4, maximum adsorbed fractions of SO_3, $a_\tau(\theta_1)$, and H_2SO_4, $a_\tau(\theta_2)$, for the three types of aircraft as explained in the text

Type	EI(soot) (g kg^{-1})	τ	θ_1	θ_2	$a_\tau(\theta_1)$	$a_\tau(\theta_2)$
1	0.4	0.013	6.7	33.3	0.042	0.076
2	0.3	0.04	2	10	0.066	0.13
3	0.6	0.2	0.4	2	0.077	0.29
ATTAS	0.025	0.0011	6.7	33.3	0.0036	0.0067

The last row gives numbers for the DLR-ATTAS aircraft based on mixing properties as for type 1 aircraft and with soot size and number density given by Kärcher et al. (1996a).

($r_s = 10$ nm). Existing aircraft/engine combinations that correspond to these types are e.g., the small subsonic DLR-ATTAS (see Schumann et al., 1996; type 1), a wide-body subsonic aircraft (type 2), and the Concorde supersonic aircraft (type 3). For all three types we find adsorption time scales $t_{ad} \simeq 0.25$ s according to Eq. (2).

Table 1 contains the required information to evaluate Eq. (13). Inspection of the fractions of SO_3 and H_2SO_4 that are adsorbed by soot, $a_\tau(\theta_1)$ and $a_\tau(\theta_2)$, respectively, already allows three important conclusions. (1) At most $\sim$ 4–8% of the emitted SO_3 are lost heterogeneously. This means that H_2SO_4 can efficiently be built up in the gas phase out of emitted SO_x since only a minor fraction of exhaust SO_3 can be removed by uptake on soot. (2) The maximum heterogeneous losses of H_2SO_4 range between $\sim$ 8–30%, leading to the conclusion that volatile gas-to-particle conversion is not limited by binary heterogeneous nucleation of H_2SO_4 and H_2O on soot, in contrast to the conjecture made by Wyslouzil et al. (1994). (3) The fraction of H_2SO_4 taken up by soot exceeds that of SO_3 by a factor of 2–4. Even if soot-induced heterogeneous oxidation of SO_3 in the presence of adsorbed H_2O would be slow (which is unlikely), the major part of S(VI) on soot is already present in the form of H_2SO_4.

We further approximate the conversion efficiency η shown in Fig. 1 for the A 310 by the simple equation

$$\eta(s) = \begin{cases} 0.01 & : \quad s \le 0.01 \\ 0.5 s^{0.85} & : \quad s > 0.01 \end{cases} \tag{14}$$

which is expected to hold approximately for types 1, 2 and 3 for an OH exit plane mixing ratio of 10 ppmv. The adsorbed mass fractions of S(VI) molecules per soot particle are shown in Fig. 4 for aircraft of type 1 (solid lines) and 3 (dashed lines), respectively, as a function of the SO_3/SO_x ratio s at emission for the range of average fuel-sulfur contents EI(S), namely 0.1 g S kg^{-1} (lower lines) up to 1 g S kg^{-1} (upper lines). The corresponding results for type 2 cases are not shown explicitly because they are quite similar to the type 3 results. If no SO_3 is emitted ($s = 0$), the total S(VI) mass that can be taken up is quite low and stays between 0.1% and 1% for both types. This changes if the fraction s of SO_x that is emitted as SO_3 exceeds a few percent due to the very efficient conversion to H_2SO_4 in these cases, cf. Fig. 1 and Eq. (14). Values of 2–10% of SO_3 produced during combustion and the subsequent turbine flow are

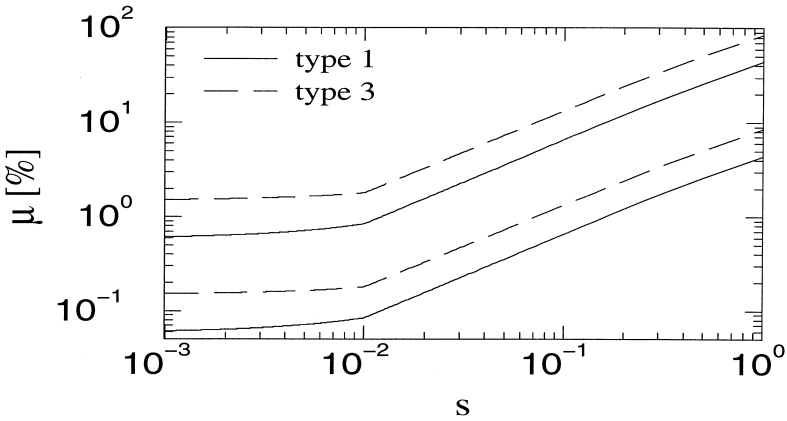

Fig. 4. Mass of adsorbed SO_3 and H_2SO_4 molecules per soot particle mass vs. $s = [SO_3]_0 / [SO_x]_0$ for the mixing specifications and soot micro-physical properties of type 1 (solid lines) and type 3 (dashed lines) aircraft (cp. Table 1). The corresponding lower and upper lines are calculated using the lower and upper limit of the average sulfur content in jet aviation fuels 0.1 g kg^{-1} and 1 g kg^{-1}, respectively, in evaluating Eq. (13). Values $\mu(s)$ for type 2 are quite similar to type 3 and are not presented explicitly. Type 3 represents cases typical for current subsonic and supersonic airliners, where adsorption is more effective than for type 1, where adsorption is limited by rapid plume mixing.

predicted by means of numerical simulations for the subsonic ATTAS and the supersonic Concorde (Brown et al., 1996). Using Fig. 4, values $s = 0.1$ translate into adsorbed mass fractions $\mu = 0.7$–7% (type 1) and $\mu = 1.4$–14% (type 3).

If the soluble mass fractions $\mu \simeq 8\%$ measured on fresh soot by Hagen et al. (1992) indeed are composed of sulfur, which seems likely because of the observed correlation of μ with the sulfur level in the kerosene (Whitefield et al., 1993), emissions of SO_3 of the order of a few percent of the total fuel sulfur are required to explain the measurements. Emission of SO_2 with subsequent conversion to H_2SO_4 alone is not sufficient to explain the measured soluble mass fractions (Kärcher et al., 1996a), in agreement with Fig. 4 for $s = 0$. The hydration measurements of single carbon aerosols performed by Wyslouzil et al. (1994) have clearly demonstrated that an average amount of adsorbed H_2SO_4 of $\sim 14\%$ on the particles was already sufficient to cause efficient wetting of the carbon surface by H_2O adsorption under water sub-saturated conditions. Putting these two facts together yields two important implications. First, to date, direct emissions of SO_3 have been ignored in numerical modeling of the aerosol formation and evolution in jet exhaust plumes (Miake-Lye et al., 1994; Kärcher, 1996). However, these models, which follow binary nucleation of H_2SO_4 and H_2O and the subsequent condensation and coagulation processes between the plume particles, suggest an extremely strong dependence of nucleation and growth rates of the volatile H_2SO_4/H_2O aerosols on $[SO_3]_0$ if $s > 10^{-2}$. This could lead to effective volatile particle emission indices and aerosol surface area densities much larger than previously thought. On a global scale, this is relevant for a proper assessment of the impact of the current and future fleet of aircraft on stratospheric ozone. Two-dimensional global models used to simulate these aircraft effects predict enhanced ozone depletion at northern midlatitudes,

if sulfur emissions are introduced into the model as volatile H_2SO_4/H_2O aerosols as compared to calculations with only gaseous SO_2 emissions and subsequent large-scale gas-to-particle conversion (Weisenstein et al., 1996). Second, the adsorbed sulfur mass is large enough to enhance the sticking probability for water molecules. On the soot surface, together with water vapor, these sulfur species nucleate heterogeneously and create a liquid soot coating, in which the presence of water may facilitate the dissociation and enhance the sticking of other soluble compounds that are present in the exhaust plume (such as HNO_2, HNO_3, or H_2O_2). Therefore, soot particles from aircraft exhaust might constitute effective ice freezing nuclei which can potentially alter natural cirrus clouds (Toon, 1995; Jensen and Toon, 1997). In the upper troposphere, homogeneous freezing of deliquescent sulfate aerosols appears to be the major cirrus-cloud-formation mechanism; heterogeneous freezing of ice in the solution triggered by soot inclusions will certainly increase the freezing rates in a given air parcel, even if soot particles are poor freezing nuclei. Related to cirrus formation, it would be interesting to know how the ice-forming ability of aircraft soot changes when the soot particles are first transformed into contrail ice and later evaporate the water vapor.

Supersaturations with respect to ice in nascent exhaust plumes can reach much higher values than in the cloud-free portions of the upper troposphere (Kärcher et al., 1996a). By analyzing the contrail experiment of Busen and Schumann (1995) performed with the DLR-ATTAS aircraft under threshold formation conditions, we concluded recently that heterogeneous freezing of the liquid soot coating has very likely caused the formation of the observed visible contrails (Kärcher et al., 1996a). Busen and Schumann (1995) have used fuels with two different sulfur levels in one single flight, one very low ($EI(S) = 0.002$ g kg^{-1}) and the other with an average mass content ($EI(S) = 0.25$ g kg^{-1}). Surprisingly, they observed no visible difference in onset and visibility of the contrails. Applying our model to the ATTAS aircraft with type 1 mixing properties as described above and with $n_{s,0} = 10^6$ cm^{-3} and $r_s = 20$ nm (cf. Table 1), we obtain $\mu(s = 0) = 2 \times 10^{-3}\%$ and $\mu(s = 0.1) = 2 \times 10^{-2}\%$ for the low fuel-sulfur case and $\mu(s = 0) = 0.2\%$ and $\mu(s = 0.1) = 2.3\%$ for the average fuel-sulfur case, see Fig. 5, the

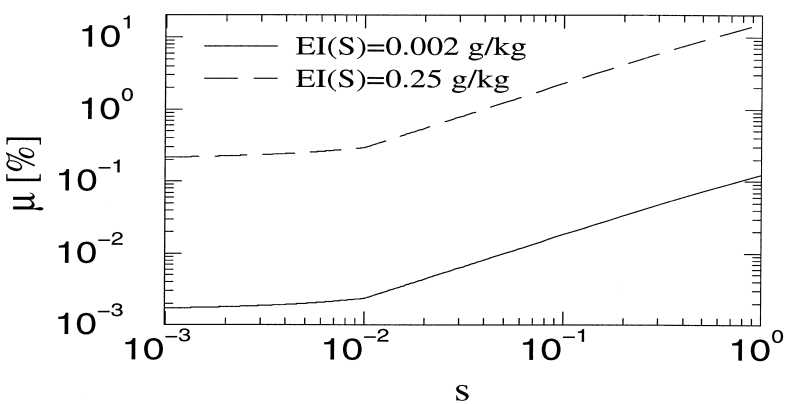

Fig. 5. As in Fig. 4, but for the DLR-ATTAS aircraft for two different fuel-sulfur contents (very low and average) as indicated in the legends.

μ-values for the $s = 0$ cases being in fair agreement with the rough estimates by Kärcher et al. (1996a). Higher values for $s > 0.1$ are also possible, but the simulations of Brown et al. (1996) for this aircraft suggest $s = 0.03$ for the average and $s = 0.06$ for the low sulfur case. Whereas it is conceivable that a liquid coating forms for EI(S) = 0.25 g kg^{-1}, where sulfur mass fractions of the order of 1% are present on the soot surface, mass fractions for EI(S) = 0.002 g kg^{-1} are quite low and one might argue that formation of such a coating does not take place, and ice formation (which took place close to liquid water saturation) was initiated by other processes in this case. However, it seems more likely that freezing of a partial liquid coating at preferred sites on the soot particles was sufficient to create enough ice particles required to make the contrail visible. Even in the low sulfur case, the number density of total sulfur at emission exceeded the background concentration by more than one order of magnitude, and it is not a priori known which degree of activation is necessary to initiate the formation of liquid solution droplets on soot. Binary heterogeneous nucleation of small H_2SO_4/H_2O droplets might become facilitated, either due to an 'inverse Kelvin law' effect in concave surface features (Pruppacher and Klett, 1978, p. 237), or because hindered diffusion in small cavities on the surface causes the molecules to stick together sufficiently long to induce the phase transition. Clearly, this somewhat speculative discussion has to be validated by experiments. In any case, the estimates for μ presented above can be used to constrain binary heterogeneous nucleation rates of H_2SO_4 and H_2O on soot under plume conditions.

5. Basic conclusions

Chemical modeling of the jet plume chemistry predicts a substantial increase in the production of gaseous H_2SO_4 in nascent exhaust plumes if more than 1% of the emitted SO_x leaves the jet engines in the form of SO_3. This dramatically enhances binary nucleation rates of new H_2SO_4/H_2O aerosols and causes a faster growth of these particles. Only a minor fraction 4–8% of exhaust SO_3 can be removed from the gas phase by uptake on soot, so that gaseous H_2SO_4 can efficiently be built up. Heterogeneous losses of H_2SO_4 range between $\sim$ 8–30%; hence, volatile gas-to-particle conversion is not limited by binary heterogeneous nucleation of H_2SO_4 and H_2O on soot. The fraction of adsorbed H_2SO_4 exceeds that of SO_3 by a factor of 2–4. If no SO_3 is emitted, the total S(VI) mass fraction on soot stays between 0.1% and 1%. For emissions of SO_3 between 1–10%, adsorbed mass fractions typically range between 0.7–14%, depending on the mixing properties of the jet plume and the initial available soot surface-area density, in better agreement with hydration measurements using fresh exhaust soot. These results might have important implications for heterogeneous chemistry in aging, stratospheric aircraft plumes and for the possible formation of cirrus clouds in the upper troposphere.

Acknowledgements

Support by the German Environmental Agency (UBA, Berlin) is gratefully acknowledged.

References

Blake, D.F., Kato, K., 1995. Latitudinal distribution of black carbon soot in the upper troposphere and lower stratosphere. J. Geophys. Res. 100, 7195–7202.

Brown, R.C., Anderson, M.R., Miake-Lye, R.C., Kolb, C.E., Sorokin, A.A., Buriko, Y.Y., 1996. Aircraft exhaust sulfur emissions. Geophys. Res. Lett. 23, 3603–3606.

Busen, R., Schumann, U., 1995. Visible contrail formation from fuels with different sulfur contents. Geophys. Res. Lett. 22, 1357–1360.

Frenzel, A., Arnold, F., 1994. Sulfuric acid cluster ion formation by jet engines: implications for sulfuric acid formation and nucleation. In: Schumann, U., Wurzel, D. (Eds.), DLR-Mitteilungen 94-06, DLR/Köln, Germany, pp. 106–112.

Fuchs, N.A., 1964. The Mechanics of Aerosols. Pergamon, Oxford.

Hagen, D.E., Trueblood, M.B., Whitefield, P.D., 1992. A field sampling of jet exhaust aerosols. Part. Sci. Technol. 10, 53–63.

Harris, B.W., 1990. Conversion of sulfur dioxide to sulfur trioxide in gas turbine exhaust. J. Eng. Gas Turb. Power 112, 585–589.

Hunter, S.C., 1982. Formation of SO_3 in gas turbines. Trans. ASME J. Eng. Power 104, 44–51.

Jensen, E., Toon, O.B., 1997. The potential impact of soot particles from aircraft exhaust on cirrus clouds. Geophys. Res. Lett. 24, 249–252.

Kärcher, B., 1995. A trajectory box model for aircraft exhaust plumes. J. Geophys. Res. 100, 18835–18844.

Kärcher, B., 1996. Aircraft-generated aerosols and visible contrails. Geophys. Res. Lett. 23, 1933–1936.

Kärcher, B., Peter, Th., 1995. Impact of aircraft emissions on stratospheric ozone: a research strategy. Phys. Chem. Earth 20, 123–131.

Kärcher, B., Peter, Th., Biermann, U.M., Schumann, U., 1996a. The initial composition of jet condensation trails. J. Atmos. Sci. 53, 3066–3083.

Kärcher, B., Hirschberg, M.M., Fabian, P., 1996b. Small-scale chemical evolution of aircraft exhaust species at cruising altitudes. J. Geophys. Res. 101, 15169–15190.

Miake-Lye, R.C., Brown, R.C., Anderson, M.R., Kolb, C.E., 1994. Calculations of condensation and chemistry in an aircraft contrail. In: Schumann, U., Wurzel, D. (Eds.), DLR-Mitteilungen 94-06, DLR/Köln, Germany, pp. 274–280.

Pitchford, M., Hudson, J.G., Hallett, J., 1991. Size and critical supersaturation for condensation of jet engine exhaust particles. J. Geophys. Res. 96, 20787–20793.

Pruppacher, H.R., Klett, J.D., 1978. Microphysics of Clouds and Precipitation. Reidel, Dordrecht.

Rogaski, C.A., Golden, D.M., Williams, L.R., 1997. Reactive uptake and hydration experiments on amorphous carbon treated with NO_2, SO_2, O_3, HNO_3, and H_2SO_4. Geophys. Res. Lett. 24, 381–384.

Schumann, U. et al., 1996. In-situ observations of particles in jet aircraft exhausts and contrails for different sulfur-containing fuels. J. Geophys. Res. 101, 6853–6869.

Stockwell, W.R., Calvert, J.G., 1983. The mechanism of the HO–SO_2 reaction. Atmos. Environ. 17, 2231–2235.

Toon, O.B., 1995. Observations—subsonic aircraft: contrail and cloud effects special study. In: Thompson, A.M., Friedl, R.R., Wesoky, H.L. (Eds.), Atmospheric Effects of Aviation: First Report of the Subsonic Assessment Project. NASA Ref. Publ. 1381, pp. 175–200.

Weisenstein, D.K., Ko, M.K.W., Sze, N.-D., Rodriguez, J.M., 1996. Potential impact of SO_2 emissions from stratospheric aircraft on ozone. Geophys. Res. Lett. 23, 161–164.

Whitefield, P.D., Trueblood, M.B., Hagen, D.E., 1993. Size and hydration characteristics of laboratory simulated jet engine combustion aerosols. Part. Sci. Technol. 11, 25–36.

World Meteorological Organization, 1995. Global Ozone Research and Monitoring Project, Report 37, Geneva.

Wyslouzil, B.E., Carleton, K.L., Sonnenfroh, D.M., Rawlins, W.T., Arnold, S., 1994. Observation of hydration of single, modified carbon aerosols. Geophys. Res. Lett. 21, 2107–2110.